

Spatial Averaging of van Genuchten Hydraulic Parameters for Steady-State Flow in Heterogeneous Soils: A Numerical Study

Jianting Zhu and Binayak P. Mohanty*

ABSTRACT

For meso- or regional-scale Soil–Vegetation–Atmosphere Transfer (SVAT) schemes in hydroclimatic models, pixel dimensions may range from several hundred square meters to several hundred square kilometers. Pixel-scale soil hydraulic parameters and their accuracy are critical for the success of hydroclimatic and soil hydrologic models. This study tries to answer a major question: What will be the effective and average hydraulic properties for the entire pixel (or footprint of a remote sensor) consisting of several textures if the soil hydraulic properties can be estimated for each individual texture? In this study, we examined the impact of areal heterogeneity in soil hydraulic parameters on soil ensemble behavior for steady-state evaporation and infiltration. Using the widely used van Genuchten model and hydraulic parameter statistics obtained from neural network–based pedotransfer functions (PTFs) for various soil textural classes, we address the impact of areal hydraulic property heterogeneity on ensemble behavior and uncertainty in steady-state vertical flow in large-scale heterogeneous fields. The various averaging schemes of van Genuchten parameters are compared with “effective parameters” calculated by conceptualizing the areally heterogeneous soil formation as an equivalent homogeneous medium that will discharge approximately the same amount of ensemble flux of the heterogeneous soil. The impact of boundary conditions and parameter correlation on the effective parameters, as well as the accuracy and uncertainty of the averaging schemes for the hydraulic parameters, are investigated and discussed. In light of our results, we suggest the following guidelines for van Genuchten hydraulic parameter averaging: arithmetic means for K_s and n , a value between arithmetic and geometric means for α when K_s and α are highly correlated, and a value between geometric and harmonic means for α when K_s and α are poorly correlated.

SPATIAL VARIABILITY in soil hydraulic parameters has been recognized for years. Because the soil hydraulic characteristics that determine unsaturated flow exhibit a large degree of spatial heterogeneity, infiltration and evaporation are spatially variable as well. Furthermore, due to the nonlinearity of the unsaturated flow equation, representation of spatial variability of upward–downward flux is a complex problem. This in turn suggests that for meso- or regional-scale Soil–Vegetation–Atmosphere Transfer (SVAT) schemes in hydroclimate models, pixel-scale soil hydraulic parameters and their accuracy are critical for the success of hydroclimate and soil hydrologic models.

Sharma and Luxmoore (1979) investigated the influence of soil variability on the water balance at a catchment scale. It was assumed in their study that soil hydraulic properties were the only variables in space and could be represented by the Miller and Miller scaling

factors. Kim and Stricker (1996) employed Monte Carlo simulation to investigate the independent and simultaneous effects of horizontal heterogeneity in soil hydraulic properties and rainfall intensity on various statistical properties of the components of the one-dimensional water budget for a large area up to 10^4 km². The effective parameters in the hydraulic property functions can be determined by inversion (e.g., Yeh, 1989) or perturbation (Milly and Eagleson, 1987; Kim et al., 1997) methods. Yeh (1989) studied the effect of soil heterogeneity on one-dimensional steady infiltration using the Gardner exponential model (Gardner, 1958) for the unsaturated hydraulic conductivity. The effective hydraulic parameters were calculated by minimizing the squared differences of the capillary pressure profiles in the formation. While the obtained parameters provided the best fit, they may not necessarily perform well in representing heterogeneous behavior of the soil because of the highly nonlinear nature of the process. Kim et al. (1997) investigated the impact of heterogeneity of the soil hydraulic properties on the spatially averaged water budget of the unsaturated zone using a framework of analytical solutions (Kim et al., 1996). Their results indicated that the “effective” set of hydraulic parameters depends on the specific climate and the spatially uniform parameters, in addition to the obvious dependence on the mean, variance, and covariances of the spatially variable parameters.

Many previous investigations of soil heterogeneity assumed so-called scaling heterogeneity (Hopmans et al., 1988; Kim and Stricker, 1996; Kim et al., 1997; Sharma and Luxmoore, 1979). Scaling theory, based on the similar media concept (Miller and Miller, 1956), provides a basis for representing soil spatial variability in terms of a single stochastic variable, the scaling factor, which is related to the microscopic characteristic length of the soil. Two soils are considered to be geometrically similar when they only differ with respect to their internal microscopic geometries.

The objectives of this study are to provide some practical guidelines of how the commonly used averaging schemes (arithmetic, geometric, or harmonic) perform when compared with the effective parameters for steady-state flow. The effective parameters are obtained by conceptualizing the heterogeneous soil formation as an equivalent homogeneous medium that will discharge approximately the same flux as the ensemble flux of the heterogeneous formations. The effective parameters so calculated are able to simulate the large-scale ensemble flux, which is a crucial quantity in modeling subsurface processes near the atmosphere and land surface interac-

B.P. Mohanty and J. Zhu, Biological and Agricultural Engineering Dep., Scoates Hall, Texas A&M University, College Station, TX 77843-2117. Received 7 Nov. 2001. *Corresponding author (bmohanty@tamu.edu).

Abbreviations: PTF, pedotransfer function; SVAT, Soil–Vegetation–Atmosphere Transfer.

tion. The commonly used simple averaging schemes are easy to use, but their appropriateness is difficult to assess given the high nonlinearity in the unsaturated zone hydrologic processes. We compare the performance of commonly used averaging schemes with the effective parameters and suggest when the simpler averaging schemes can be used in lieu of the effective parameters. Using the widely used van Genuchten model along with the neural network-based PTFs for hydraulic parameter estimations based on several large soil databases, we address the impact of areal hydraulic property heterogeneity on ensemble behavior and uncertainty in steady-state vertical flow in large-scale heterogeneous fields with various soil textures. Experimental characterization of the hydraulic parameters for large areas can be very expensive and time-consuming. Moreover, complete deterministic characterization of many fields is generally not possible due to spatial variability. An increasingly popular alternative to direct measurement of the unsaturated soil hydraulic properties of soils is to use PTFs. Pedotransfer functions transform simple soil properties such as texture, bulk density, and other soil pedon information into soil water retention and saturated or unsaturated hydraulic conductivity information (e.g., Wosten and van Genuchten, 1988; Schaap and Leij, 1998). In this study, we adopt the statistics for the van Genuchten parameters (K_s , α , and n) from a neural network-based PTF of Schaap and Leij (1998) derived from three large databases for different USDA textural classes. The statistics (mean and standard deviation) so derived are used in this study to generate random fields of van Genuchten parameters for different textural classes.

For meso- or regional-scale SVAT schemes in hydroclimatic models, pixel dimensions may range several hundred square meters to several hundred square kilometers, while the vertical scale of subsurface processes near the atmosphere and surface interaction is considerably small. In such a large horizontal scale, the areal heterogeneity of hydraulic properties dominates compared with the heterogeneity at (much smaller) vertical scale. Therefore, it is reasonable to consider only the areal heterogeneity, while ignoring vertical heterogeneity. In treating such areal heterogeneity for the scenario of steady-state flow, we adopt the stream-tube assumption, which assumes that the flow is virtually vertical for each cell with no flow in the horizontal direction. Therefore, we made two major assumptions in this study: (1) hydraulic parameter heterogeneity is limited to the horizontal direction and (2) flow is limited to the vertical direction. These two assumptions seem to be contradictory since the assumption of horizontal heterogeneity would result in different pressure profiles across different cells within a pixel, which in turn would lead to horizontal flow induced by the pressure differentials across different cells or stream tubes. To validate our assumption (2), we further calculated the maximum ratio of horizontal flux rate over vertical flux rate for a typical pixel dimension.

THEORY

van Genuchten Hydraulic Property Model and Pedotransfer Functions

van Genuchten Model

Some of the more commonly used models describing the relationship between the water content (θ) and the capillary pressure head (ψ), and the relationship between the unsaturated hydraulic conductivity (K) and the capillary pressure head include the van Genuchten (1980) model, the Brooks–Corey model (Brooks and Corey, 1964), and the Gardner–Russo model (Gardner, 1958; Russo, 1988). Although many spatial variability analyses have utilized the Gardner–Russo model because of its simplicity, this model may not fit the measured $K(\psi)$ and $\theta(\psi)$ relationships for the entire range of ψ (e.g., Leij et al., 1997). We use the model of van Genuchten (1980), which closely fits measured water-retention data of many types of unstructured soils (Leij et al., 1997). Van Genuchten's model for the soil water retention curve combined with the hydraulic conductivity function (Mualem, 1976) can be expressed as follows,

$$S_e(\psi) = \frac{1}{[1 + (\alpha\psi)^n]^m} \quad [1]$$

$$K(\psi) = \frac{K_s \{1 - (\alpha\psi)^m [1 + (\alpha\psi)^n]^{-m/2}\}^2}{[1 + (\alpha\psi)^n]^{m\ell}} \quad m = 1 - 1/n \quad [2]$$

where $S_e = (\theta - \theta_r)/(\theta_s - \theta_r)$ is the relative saturation or the reduced water content ($0 \leq S_e \leq 1$), the subscripts "s" and "r" refer to saturated and residual values, and where α , n , and m are parameters that determine the shape of the soil water retention curve. K_s is the saturated hydraulic conductivity and ℓ is a pore-connectivity parameter. Note that parameter ℓ estimated to be about 0.5 as an average for many soils (Mualem, 1976) was used in this study. However, more recent studies (e.g., Wosten and van Genuchten, 1988; Schuh and Cline, 1990; Yates et al., 1992; Schaap and Leij, 1998) suggest that other values of ℓ may represent the hydraulic behavior of many soils equally well or better.

Experimental characterization of the van Genuchten hydraulic parameters for large areas can be very expensive and time-consuming. Besides, complete deterministic characterization of many fields is generally not possible because of spatial variability. This has led to the treatment of those parameters as spatially stochastic parameters.

Pedotransfer Functions and Parameter Uncertainties

An increasingly popular alternative to direct measurement of the unsaturated soil hydraulic properties of soils is to use PTFs. Pedotransfer functions transform simple soil properties such as texture, bulk density, and other soil pedon data into soil water retention and saturated or unsaturated hydraulic conductivity information (Wosten and van Genuchten, 1988; Schaap and Leij, 1998). Schaap and Leij (1998) developed hierarchical neural network-based PTFs to predict parameters in the retention function of van Genuchten (1980) and the saturated hydraulic conductivity, K_s . Three large databases (i.e., RAWLS, AHUJA, and UNSODA [Leij et al., 1996]) were employed to evaluate the accuracy and uncertainty of neural network-based PTFs. Schaap and Leij (1998) investigated the accuracy and reliability of the PTF predictions using calibration, validation, and cross-validation of the neural network-based PTFs combined with the bootstrap method. Table 1 lists the averages and the standard deviations of α and K_s for different USDA textural classes (Schaap and Leij, 1998). The

Table 1. Mean values of K_s , α , and n for different textural classes. Standard deviations are given in parentheses (extracted from Schaap and Leij, 1998).

Class	$N_{\alpha&n}^\dagger$	$\log(\alpha)$	$\log(n)$	$N_{K_s}^\dagger$	$\log(K_s)$
		$\log(\text{cm}^{-1})$			$\log(\text{cm d}^{-1})$
Sand	308	-1.45(0.25)	0.50(0.18)	253	2.81(0.59)
Loamy sand	205	-1.46(0.47)	0.24(0.16)	167	2.02(0.64)
Loam	249	-1.95(0.73)	0.17(0.13)	113	1.08(0.92)
Sandy loam	481	-1.57(0.45)	0.16(0.11)	314	1.58(0.66)
Silt loam	332	-2.30(0.57)	0.22(0.14)	135	1.26(0.74)
Sandy clay loam	181	-1.68(0.71)	0.12(0.12)	135	1.12(0.85)
Silty clay loam	89	-2.08(0.59)	0.18(0.13)	40	1.05(0.76)
Clay loam	150	-1.80(0.69)	0.15(0.12)	62	0.91(1.09)
Silt	6	-2.18(0.30)	0.22(0.13)	3	1.64(0.27)
Clay	92	-1.82(0.68)	0.10(0.07)	60	1.17(0.92)
Sand clay	12	-1.48(0.57)	0.08(0.06)	10	1.06(0.89)
Silty clay	29	-1.79(0.64)	0.12(0.10)	14	0.98(0.57)

† Number of samples per textural class.

values are used in this study to generate random fields of α , K_s , and n for different textural classes. Given those statistical properties based on a PTF from a large soil database and wide range of possible correlations of two random fields, the random fields generated are quite reasonable represent wide range of actual field scenarios.

Steady-State Vertical Flow at Local Scale and Parameter Averaging Schemes

Steady-State Evaporation and Infiltration at Local Scale

At local scale, the pressure profile during one-dimensional steady-state unsaturated capillary flow without macropore and root water uptake, can be written as (e.g., Zaslavsky, 1964; Warrick and Yeh, 1990)

$$z = \int_0^\psi \frac{K(\psi)d\psi}{K(\psi) + q} \quad [3]$$

where z is the vertical distance (positive upward) with the water table location being at $z = 0$, and q is the evaporation (positive) or infiltration (negative) rate. Its dimensionless form can be expressed as

$$\alpha z = \int_0^{\alpha\psi} \frac{K_r(x)dx}{K_r(x) + q'} \quad [4]$$

where the dimensionless hydraulic conductivity $K_r = K/K_s$, the dimensionless pressure head $x = \alpha\psi$, and the dimensionless flux rate $q' = q/K_s$. When the pressure head at the surface, P_s , is known, the dimensionless steady-state flux q' can be found out from the following equation

$$\alpha L = \int_0^{\alpha P_s} \frac{K_r(x)dx}{K_r(x) + q'} \quad [5]$$

where L is the elevation of the ground surface above the water table. From Eq. [5], it can be seen that the dimensionless steady-state flux rate q' itself is not related to the saturated hydraulic conductivity K_s . In other words, the flux rate q is a linear function of K_s . Since there is a linear relationship between the flux and the saturated hydraulic conductivity, the arithmetic mean for the K_s is deemed adequate.

Averaging Schemes for Hydraulic Properties

The parameters K_s and α can be satisfactorily fit using lognormal distributions (Smith and Diekkruger, 1996; Nielsen et al., 1973). In this study, both K_s and α are assumed to

obey the lognormal distribution. Since the van Genuchten parameter n has to be greater than 1 (van Genuchten and Nielsen, 1985), we assume $(n - 1)$ rather than n to be lognormally distributed; this ensures that $n > 1$ when considering spatial variability in n . The cross-correlated random fields of the parameters K_s , α , and $n - 1$ were generated using the spectral method proposed by Robin et al. (1993) and the resulting FORTRAN computer code FGEN (J.L. Wilson, 1995, personal communication). Random fields were produced with the power spectral density function, which was based on exponentially decaying covariance functions. The coherency spectrum, given by Eq. [6], is an indicator of parameter correlation,

$$R(\mathbf{f}) = \frac{\phi_{12}(\mathbf{f})}{[\phi_{11}(\mathbf{f})\phi_{22}(\mathbf{f})]^{1/2}} \quad [6]$$

where $\phi_{11}(\mathbf{f})$ and $\phi_{22}(\mathbf{f})$ are the power spectra of random fields $\log(K_s)$ and $\log(\alpha)$ or $\log(K_s)$ and $\log(n - 1)$, respectively, $\phi_{12}(\mathbf{f})$ is the cross spectrum between $\log(K_s)$ and $\log(\alpha)$ or $\log(K_s)$ and $\log(n - 1)$. Having $|R|^2 = 1$ indicates perfect linear correlation between the random fields. The random fields are assumed to be isotropic, with the domain length being equal to 10 correlation lengths, which in turn corresponds to 50 grid lengths. A random field of 2500 (50×50) values was generated for $\log(K_s)$, $\log(\alpha)$ or $\log(n - 1)$ field. Given those statistical properties based on the PTF from the large soil database (Schaap and Leij, 1998) and wide range of possible correlation of two random fields, the random fields generated are quite reasonable, representing a wide range of actual field scenarios.

We will investigate two main themes of hydraulic parameter spatial variability when calculating dynamic flow characteristics in a heterogeneous unsaturated soil: (i) a variable saturated hydraulic conductivity K_s and a variable van Genuchten parameter α , with a constant van Genuchten parameter n , or (ii) a variable saturated hydraulic conductivity K_s and a variable n , with a constant α . We will consider these two scenarios separately to investigate the respective impacts of their spatial heterogeneity. For each theme we consider three hydraulic parameter averaging schemes and compare them with effective parameters calculated according to the ensemble flux behavior, that is, the mean behavior of the flow dynamics. The hydraulic parameter averaging schemes considered are: (i) arithmetic means for both the spatial variables, (ii) arithmetic means for K_s and geometric means for α or n ; and (iii) arithmetic means for K_s and harmonic means for α or n . As discussed above, for the nature of areally heterogeneous vertical flow we consider in this study, the arithmetic average (mean) for the saturated hydraulic conductivity can be considered as an appropriate averaging scheme. For the following numerical experiments showing results for dynamic flow, we

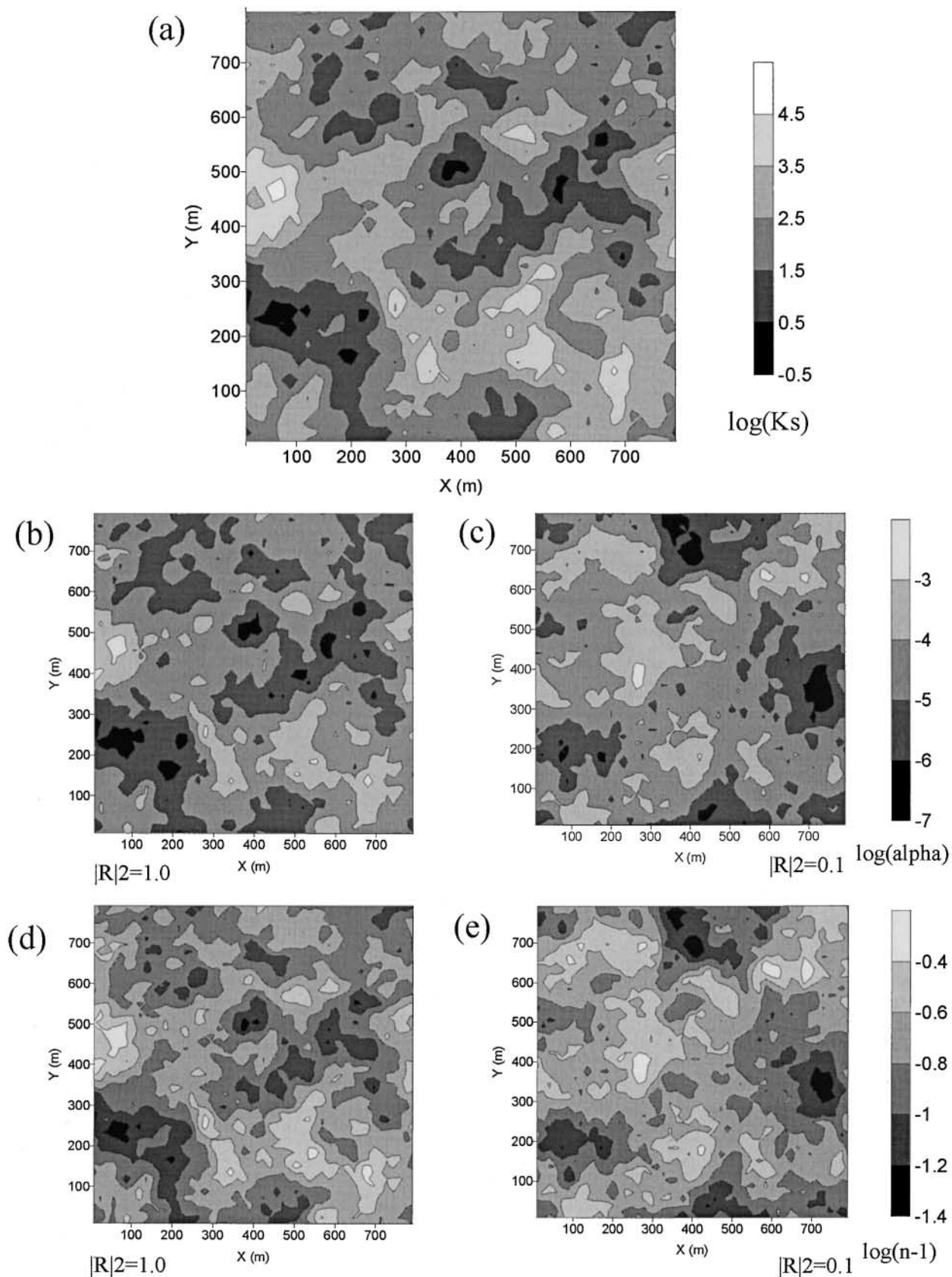


Fig. 1. Images of randomly generated van Genuchten parameter fields for loam used in the simulations. (a) $\log(K_s)$ with K_s in centimeters per day; (b) $\log(\alpha)$ with α in (1/cm), $|R|^2 = 1.0$; (c) $\log(\alpha)$ with α in (1/cm), $|R|^2 = 0.1$; (d) $\log(n - 1)$, $|R|^2 = 1.0$; (e) $\log(n - 1)$, $|R|^2 = 0.1$.

used a shallow water table depth of 180 cm, typical of semiarid and semihumid regions.

RESULTS AND DISCUSSION

Several representative images of randomly generated van Genuchten parameter fields for $\log(K_s)$, $\log(\alpha)$, and $\log(n-1)$ used in the simulations are shown in Fig. 1. The input means and the standard deviations are based on the values for the loam soil in Table 1 and on assuming exponentially decayed covariance functions. Figure 1a represents spatially variable $\log(K_s)$ values with K_s in centimeters per day. Figure 1b shows plots of $\log(\alpha)$ with α (in 1/cm) fully correlated with the $\log(K_s)$ field (i.e., $|R|^2 = 1.0$), while Fig. 1c represents $\log(\alpha)$ when $|R|^2 = 0.1$. Similarly, Fig. 1d is for $\log(n-1)$ when it is fully correlated with $\log(K_s)$ (i.e., $|R|^2$ between $\log(K_s)$ and $\log(n-1)$ is 1.0), while Fig. 1e represents $\log(n-1)$ when $|R|^2 = 0.1$. As expected, when the two random fields are fully correlated, their images follow very similar patterns (compare Fig. 1a and 1b as well as 1a and 1d), while the other images (i.e., Fig. 1c and 1e) for much lower degrees of correlation have little resemblance with the $\log(K_s)$ image (i.e., Fig. 1a).

Figure 2 plots the corresponding $\log(q)$ fields with

q in centimeters per second for both infiltration and evaporation calculated using as input the parameter distributions of Fig. 1 when K_s and α are assumed to be spatially variable fields. The surface pressure head, P_s , is the negative of suction at the soil surface. Left-hand images (Fig. 2a and 2c) are results for the infiltration flux, while the right-hand images (Fig. 2b and 2d) are for the evaporative flux rate. The top images (Fig. 2a and 2b) represent results when the two spatially variable fields, $\log(K_s)$ and $\log(\alpha)$, are fully correlated (i.e., $|R|^2 = 1.0$), while the bottom images (Fig. 2c and 2d) are for $|R|^2 = 0.1$. In general, a larger K_s would lead to a larger flux rate, while a larger α or n would result in a smaller rate. Notice that the infiltration flux rate is mainly determined by the saturated hydraulic conductivity field, K_s . The infiltration flux rate is typically larger when K_s is larger (compare Fig. 2a and 2c with Fig. 1a). The evaporative flux rate is mainly determined by the α field. The evaporative flux is typically larger when α is smaller (compare Fig. 2b with Fig. 1b and Fig. 2d with Fig. 1c). For both infiltration and evaporation, the flux field is less variable when two random parameter fields are more correlated; that is, the variation range of $\log(q)$ is significantly smaller when $|R|^2 = 1.0$ as compared to

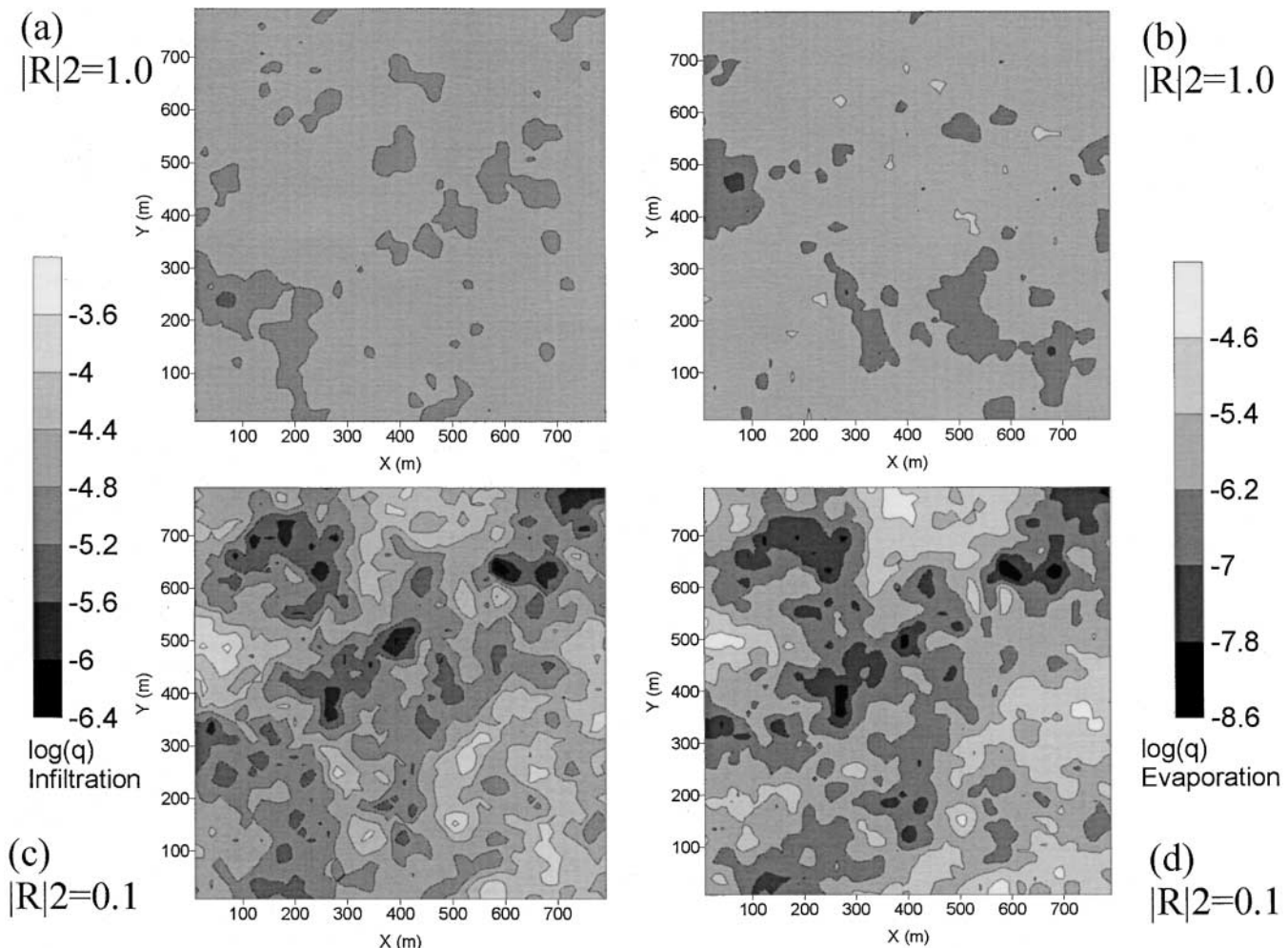


Fig. 2. Calculated $\log(q)$ fields with q in centimeters per second for both infiltration and evaporation when K_s and α are spatially variable fields. (a) Infiltration with $|R|^2 = 1.0$; (b) evaporation with $|R|^2 = 1.0$; (c) infiltration with $|R|^2 = 0.1$; (d) evaporation with $|R|^2 = 0.1$. $P_s = 30$ (-cm) for infiltration and $P_s = 480$ (-cm) for evaporation.

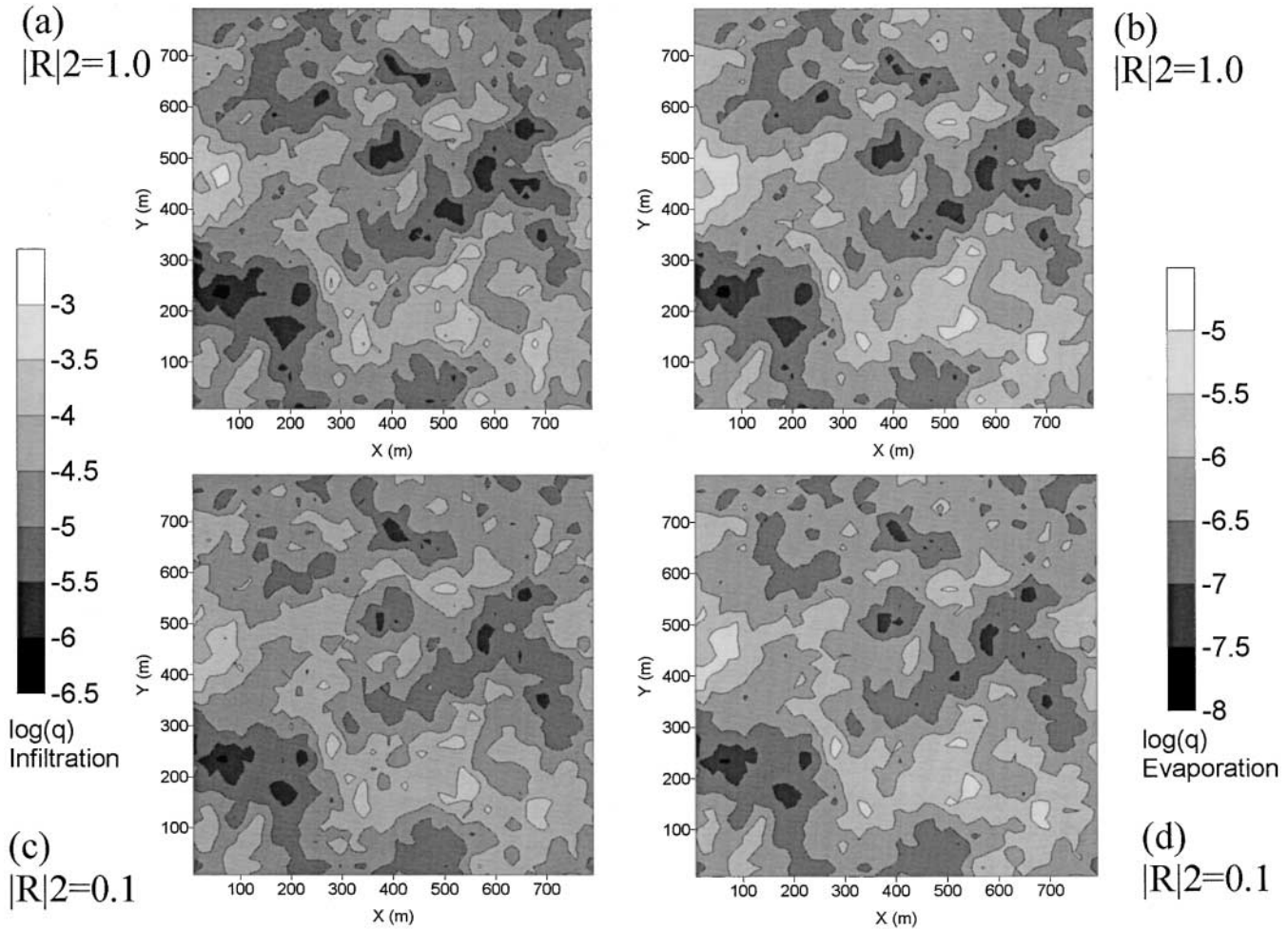


Fig. 3. Calculated $\log(q)$ fields with q in centimeters per second for both infiltration and evaporation when K_s and $n - 1$ are spatially variable fields. (a) Infiltration with $|R|^2 = 1.0$; (b) evaporation with $|R|^2 = 1.0$; (c) infiltration with $|R|^2 = 0.1$; (d) evaporation with $|R|^2 = 0.1$. $P_s = 30$ (-cm) for infiltration and $P_s = 480$ (-cm) for evaporation.

$|R|^2 = 0.1$ (compare Fig. 2a with Fig. 2c and Fig. 2b with Fig. 2d). The reduced variability in the flux field due to correlation of the K_s and α fields can be better understood by considering the separate effects of K_s and α on the flux and the implication of the correlation between K_s and α . A larger K_s would lead to a larger flux rate, while a larger α (i.e., inversely proportional to the bubbling pressure) would result in a smaller rate. A higher degree of correlation between K_s and α means that the values K_s and α in each cell would be either simultaneously high or low, thus nullifying the effect of each other and leading to reduced flux variability across the cells seen in Fig. 2a and Fig. 2b. Therefore, the variability in the flux rate is significantly larger when the two fields are negligibly correlated. Using the same reasoning, one would expect an even larger variability in the flux field in the unlikely event of a negative correlation between K_s and α .

Figure 3 plots the corresponding $\log(q)$ fields with q in centimeters per second for both infiltration and evaporation calculated using the input parameters of Fig. 1 when K_s and $n - 1$ are assumed to be spatially variable fields. It can be seen that all flux field images follow the pattern of the K_s field, with a larger K_s re-

sulting in a larger flux. The main reason for this is that the variance of $\log(n)$ is quite small compared with that of K_s , while its variability is not large enough to have a significant impact on the flux field. In practice, the parameter n can be determined with greater certainty than the other parameters involved in van Genuchten model (e.g., Schaap and Leij, 1998). From a physical perspective, α in the van Genuchten equation relates to the mean pore size magnitude, whereas n relates to the degree of pore size spreading. In their study relating the van Genuchten hydraulic property model, Hills et al. (1992) also demonstrated that the random variability in water retention characteristics could be adequately modeled using either a variable parameter α with a constant parameter n , or a variable n with a constant α , with better results when α was variable. As we have explained, Fig. 3 (infiltration and evaporation when K_s and $n - 1$ are the spatial variables) follows the pattern of K_s , while for Fig. 2 (infiltration and evaporation when K_s and α are the spatial variables), infiltration follows the K_s pattern and evaporation follows the inverse α pattern. Figure 2b is for evaporation when K_s and α are fully correlated, which follows the inverse α pattern. In

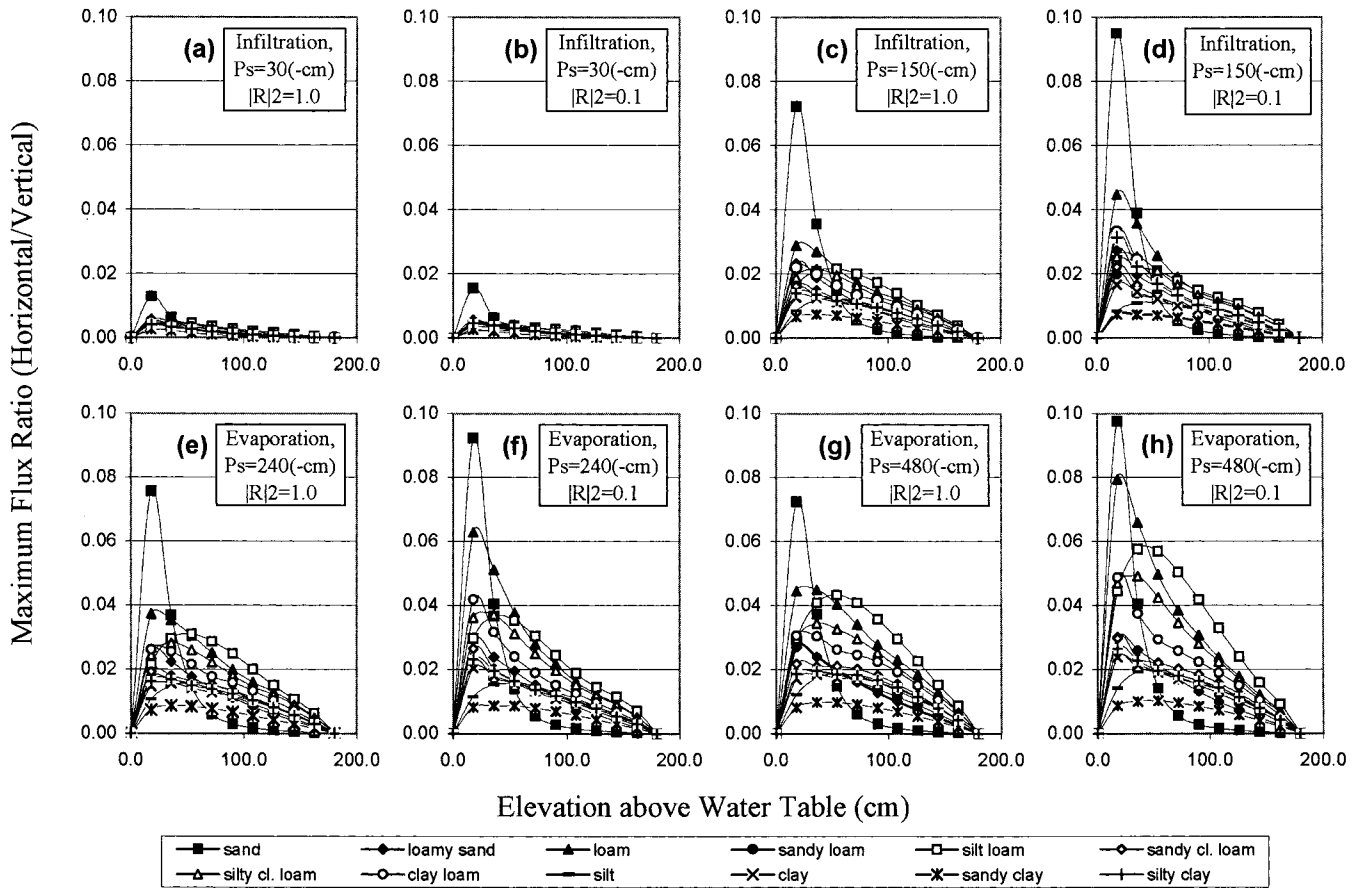


Fig. 4. Maximum ratio of the horizontal flux over the vertical flux (q_h/q) for selected values of the surface pressure head when K_s and α are spatially variable fields.

other words, it follows the inverse K_s pattern, as can be seen by comparing Fig. 3 with Fig. 2b.

The maximum ratio of horizontal flux rate over vertical flux rate used in the plots is defined as follows

$$\text{Max}\left(\frac{q_h}{q}\right) = \text{Max}_{i,j} \left[\frac{K_{ij} |\psi_{i+1,j} - \psi_{i-1,j}|}{|q_{ij}| 2\Delta x}, \frac{K_{ij} |\psi_{i,j+1} - \psi_{i,j-1}|}{|q_{ij}| 2\Delta y} \right] \quad [7]$$

where $(\Delta x, \Delta y)$ is the cell size, q_{ij} is the evaporation or infiltration rate of cell (i, j) , and K_{ij} is the unsaturated hydraulic conductivity of cell (i, j) . In the calculations, the cell size was assumed to be 16 by 16 m, which means 2500 cells or stream tubes existed in an 800 by 800 m pixel. A length of 80 m has been used for the correlation length, which means both Δx and Δy are 1/5 of the correlation length. The horizontal flux rate was calculated as the flow rate induced by the pressure differential between two alternate cells and the hydraulic conductivity at a local depth.

Plotted in Fig. 4 are the maximum ratios of the horizontal flux over the vertical flux (q_h/q) for selected values of the surface pressure head (P_s) when K_s and α are assumed to be spatially variable fields. Figure 4a, 4c, 4e, and 4g represent results when the two random fields are fully correlated ($|R|^2 = 1.0$), while Fig. 4b, 4d, 4f, and 4h show the results for $|R|^2 = 0.1$. The top four plots are for infiltration, while the bottom four figures are

for evaporation. When K_s and α are spatially variable, sand always produced the largest maximum ratio of horizontal over vertical flows in comparison with other textural classes. The maximum ratio (q_h/q) typically appeared close to the water table. The location at which the ratio reached the maximum, z_{max} , is related to the height of the capillary fringe for each individual soil textural class. From the figures we note that the silt loam class has the largest z_{max} , which leads to the smallest mean value of α (or the highest mean capillary fringe). A higher capillary fringe would mean a larger hydraulic conductivity at a higher location, a condition that would favor more horizontal flow. Another distinct feature seen from the figures is that infiltration at low surface pressure heads (Fig. 4a and 4b) leads to the low horizontal and vertical flow ratios (no larger than 2%). This is a result of diminishing pressure differentials across different cells as the flow scenario switches from large surface pressures to small surface pressures. The free drainage scenario is an extreme case where pressure gradient across the formation, including at the surface, is always zero, which means no horizontal flow between cells. The same is true when K_s and $n - 1$ are spatially variable, as shown in Fig. 5a and 5b.

Similar to Fig. 4, Fig. 5 plots maximum ratios of the horizontal flux over the vertical flux for selected values of the surface pressure head when K_s and $n - 1$ are spa-

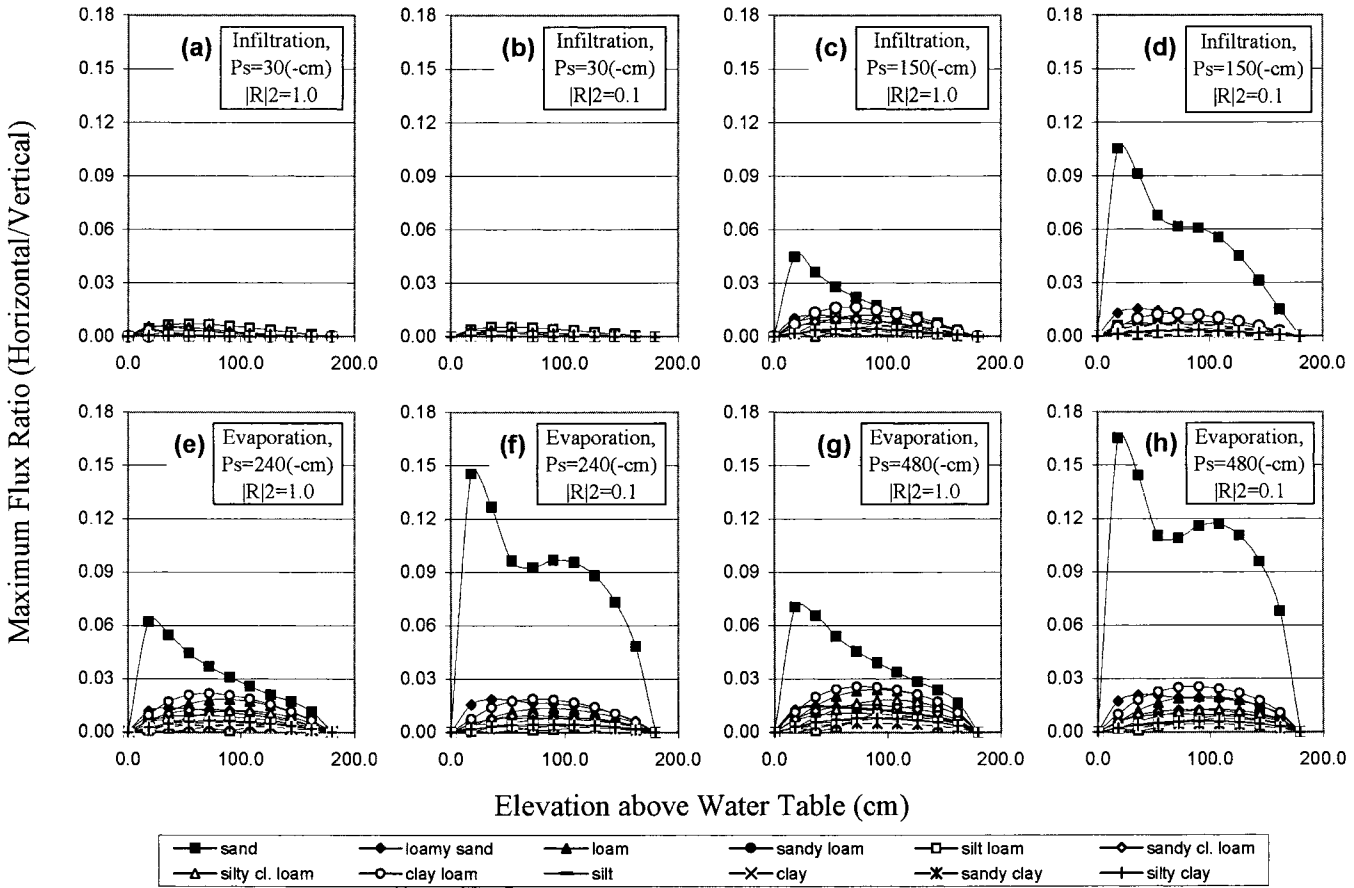


Fig. 5. Maximum ratio of the horizontal flux over the vertical flux (q_h/q) for selected values of surface pressure head when K_s and $n - 1$ are spatially variable fields.

tially variable fields. Figure 5a, 5c, 5e, and 5g represent results when the two random fields are fully correlated ($|R|^2 = 1.0$), while Fig. 5b, 5d, 5f, and 5h show results for $|R|^2 = 0.1$. Again, the results are for infiltration and evaporation. When K_s and $n - 1$ are variable, the sand class also produced the largest maximum (q_h/q) ratio, except for the condition of a small surface pressure head, which means a situation close to free drainage. For the small surface pressure condition, silt loam produced the largest maximum (q_h/q) ratio. From Table 1 we can see that the silt loam class has the smallest α or largest air-entry pressure head, that is, the largest capillarity. The maximum ratio is expected to be related to variance (variability) in hydraulic parameters and the soil textural class (mean hydraulic parameter values). Figures 4 and 5 indicate that the maximum ratio (q_h/q) is quite small and no more than 17% for all cases, thus supporting the hypothesis that the stream-tube type of flow assumption used in this study is reasonable assumption, while making our analysis significantly more tractable. Note that, in calculating the results for Fig. 4 and 5, a depth increment of 9 cm was used, although the increment used for the plots is 18 cm.

The effective parameter α_{eff} as a function of the surface pressure head for various soil textural classes is plotted in Fig. 6. Notice that α_{eff} decreases as the value of surface pressure head increases (or as flow switches from infiltration to evaporation). High correlation be-

tween K_s and α results in consistently large effective parameter α_{eff} . These results are consistent with our previous findings that correlation between K_s and α makes the soil more sand-like, that is, having large effective parameter α_{eff} (Zhu and Mohanty, unpublished data). Although variability of q is smaller as a result of parameter correlation, it makes ensemble behavior more sand-like. A reasonable practical guide for most soil textural classes is that the effective α falls between the arithmetic mean and the geometric mean for the highly correlated case, and between the geometric mean and the harmonic mean for the less correlated case, with the exception of two coarser textural classes (loamy sand and sand). For infiltration, the effective value would be near the top limit of that range.

Figure 7 plots for various soil textural classes the effective parameter n_{eff} as a function of the surface pressure head. The influence of surface pressure head on n_{eff} is not as strong as on α_{eff} . This is partly because the variance of $\log(n)$ is small. The higher correlation between K_s and $n - 1$ usually leads to a slightly larger effective parameter n_{eff} . Hence, the results also demonstrate that correlation between K_s and $n - 1$ makes the soil more sand-like (i.e., giving a larger effective parameter n_{eff}). The effect, however, is typically small. For practical applications it will be reasonable to ignore the effect of spatial variability in the parameter n , given its small impact on the effective values, and the fact

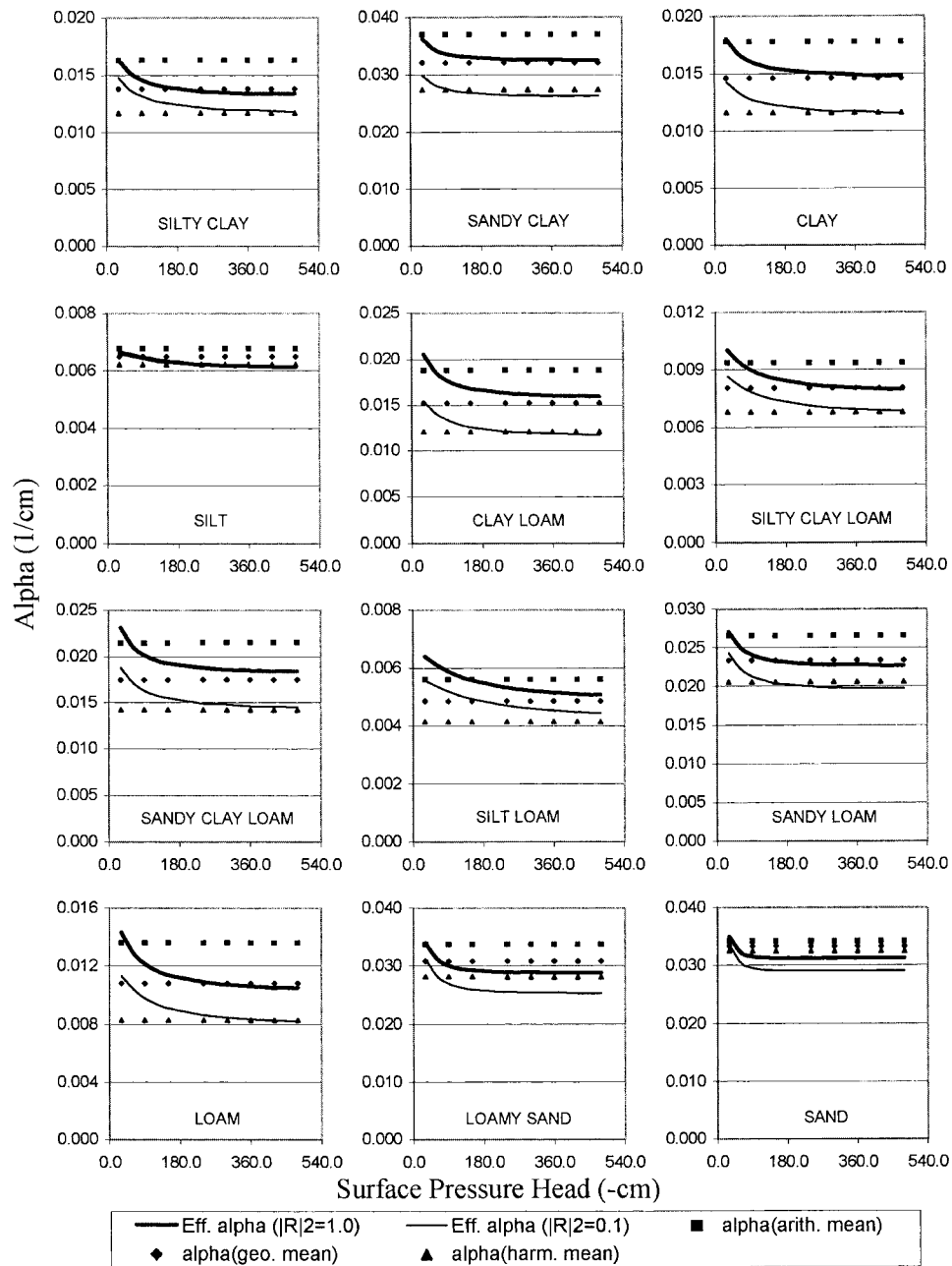


Fig. 6. Effective parameter α_{eff} vs. surface pressure for various soil textural classes.

that it can be determined with greater certainty than the other parameters in van Genuchten's model, as mentioned above.

The coefficient of variation in the flux against the surface pressure head for various soil textural classes are shown in Fig. 8. When K_s and α are correlated, the flux field is significantly less variable (i.e., having smaller coefficients of variation). The result is consistent with what can be observed from Fig. 2 as discussed above. When K_s and $n - 1$ are correlated, the q field is usually slightly more variable (i.e., having larger coefficients of variation), with the exception of relatively coarse soils (notably sand, loamy sand, and sandy loam). When K_s and α are assumed to be spatially variable, the coefficient of variation in the q field systematically increases

as the value of surface pressure head increases over a wide range of values covering both infiltration and evaporation. When K_s and $n - 1$ are assumed to be spatially variable, the effect of a varying surface pressure head on the coefficient of variation of the q field is less significant as compared with the case when K_s and α are assumed to be spatially variable.

CONCLUSIONS

The following major conclusions can be drawn from this study:

1. Spatial variability in α has a larger impact on the ensemble behavior of soils than does n , partly be-

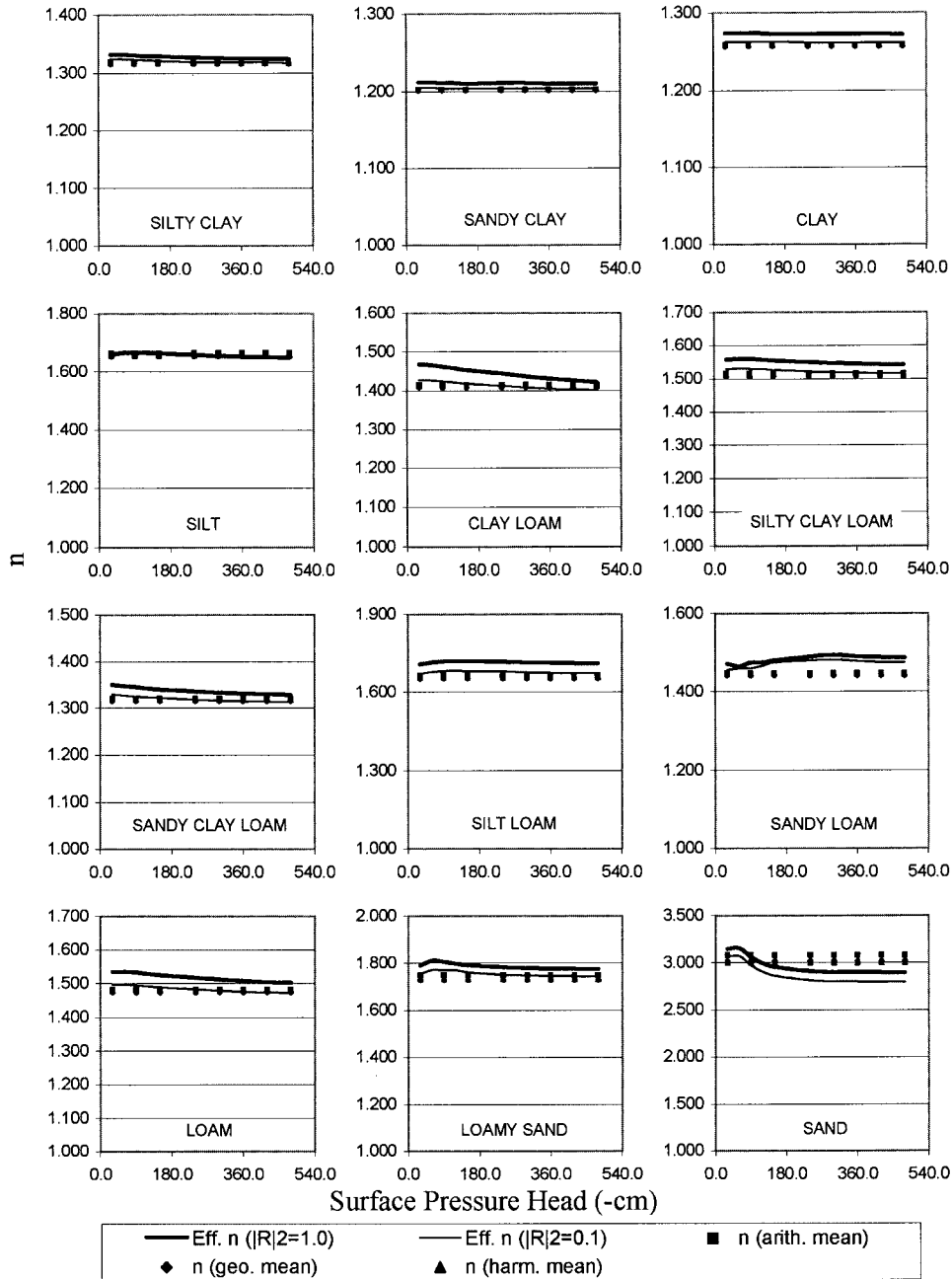


Fig. 7. Effective parameter n_{eff} vs. surface pressure for various soil textural classes.

cause n can be determined with greater certainty in practice as can be observed in Table 1. Therefore, it is reasonable to treat n as deterministic.

2. Our study suggested that we are still able to use the same form of hydraulic conductivity function for the local scale as for large-scale modeling. For the large-scale modeling, we need to use the effective hydraulic conductivity parameters, which are variable according to the boundary conditions. For coarse-textured fields, it is more difficult to define “average parameters” in lieu of “effective parameters” to simulate ensemble soil behavior, since the effective parameters tend to change more rapidly with surface pressure conditions.
3. With appropriately selected schemes, hydraulic pa-

rameter averaging performs better for simulating capillary phenomenon of relatively fine-textured soils, but is less successful for simulating the smoother ensemble profile of gradual transition.

4. For typical applications in hydrologic and hydroclimate models, the assumption of stream-tube type vertical flow for large fields is reasonable since horizontal pressure discontinuities would cause little horizontal flow as compared with vertical flow.

Results of this study suggest the following practical guidelines for averaging van Genuchten parameters when dealing with large-scale steady-state infiltration and evaporation: arithmetic means for K_s and n , values between the arithmetic and geometric means for α when K_s and α are highly correlated, and values between the geomet-

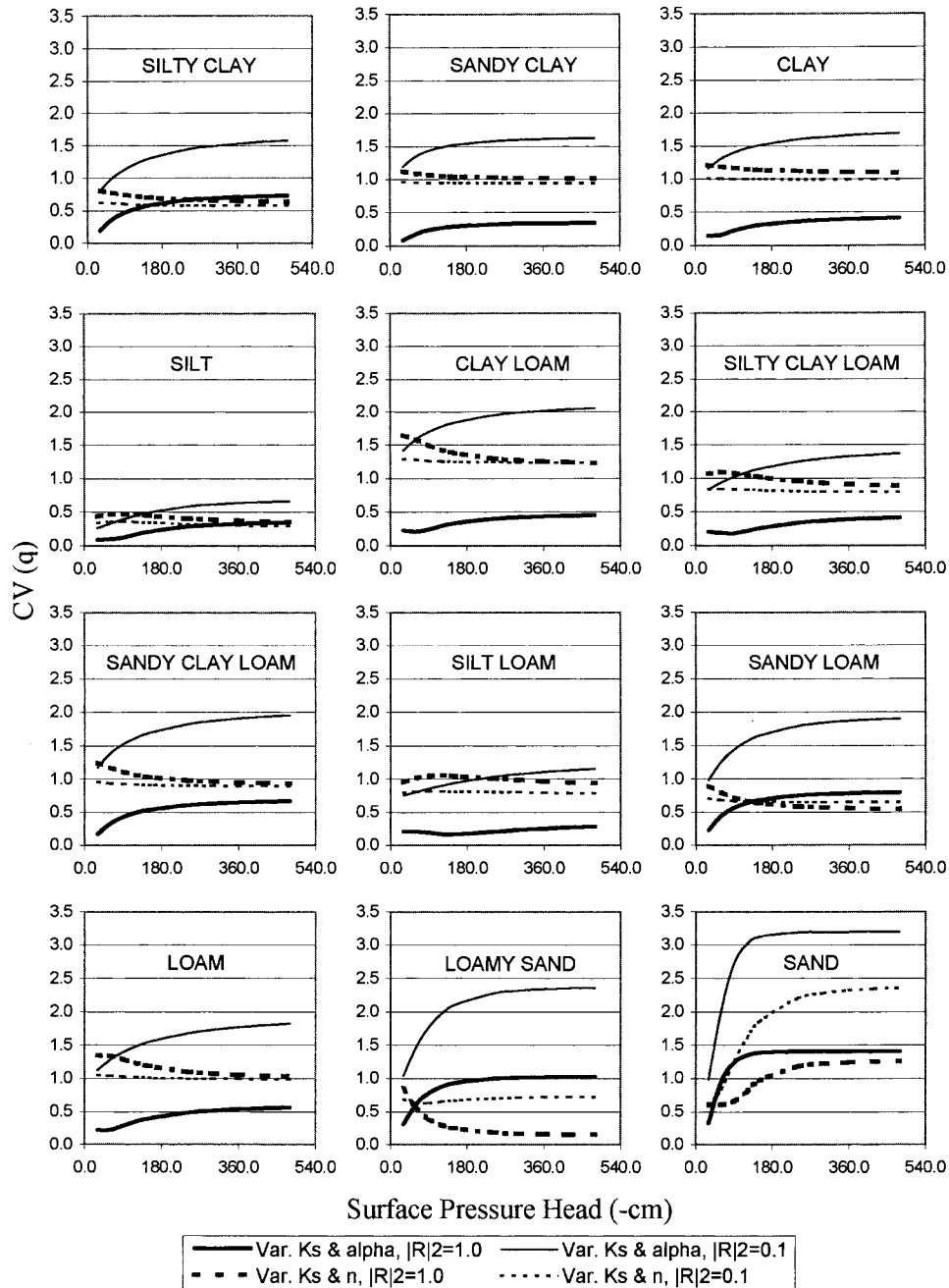


Fig. 8. Coefficient of variation of the flux against surface pressure head for various soil textural classes.

ric and harmonic means for α when K_s and α are only little correlated.

ACKNOWLEDGMENTS

This project was supported by NASA (grant No. NAG5-8682) and NSF-SAHRA at the University of Arizona. This work was initiated when the authors were at the George E. Brown Salinity Laboratory, Riverside, CA. The authors would like to thank Dr. J.L. Wilson of New Mexico Institute of Mining and Technology who provided the random field generation code.

REFERENCES

Brooks, R.H., and A.T. Corey. 1964. Hydraulic properties of porous media. Hydrology Paper 3. Colorado State Univ., Fort Collins, CO.

Gardner, W.R. 1958. Some steady state solutions of unsaturated moisture flow equations with applications to evaporation from a water table. *Soil Sci.* 85:228-232.
 Hills, R.G., D.B. Hudson, and P.J. Wierenga. 1992. Spatial variability at the Las Cruces trench site. p. 529-538. *In* M.Th. van Genuchten et al. (ed.) Indirect methods for estimating the hydraulic properties of unsaturated soils. Univ. of California, Riverside, CA.
 Hopmans, J.W., H. Schukking, and P.J.J.F. Torfs. 1988. Two-dimensional steady state unsaturated water flow in heterogeneous soils with autocorrelated soil hydraulic properties. *Water Resour. Res.* 24:2005-2017.
 Kim, C.P., and J.N.M. Stricker. 1996. Influence of spatially variable soil hydraulic properties and rainfall intensity on the water budget. *Water Resour. Res.* 32:1699-1712.
 Kim, C.P., J.N.M. Stricker, and R.A. Feddes. 1997. Impact of soil heterogeneity on the water budget of the unsaturated zone. *Water Resour. Res.* 33:991-999.
 Kim, C.P., J.N.M. Stricker, and P.J.J.F. Torfs. 1996. An analytical

- framework for the water budget of the unsaturated zone. *Water Resour. Res.* 32:3475–3484.
- Leij, F.J., W.J. Alves, M.Th. van Genuchten, and J.R. Williams. 1996. The UNSODA unsaturated soil hydraulic database. Version 1.0. Report IAG-DW 12933934. National Risk Management Research Laboratory, Office of Research and Developments. USEPA, Cincinnati, OH.
- Leij, F.J., W.B. Russell, and S.M. Lesch. 1997. Closed-form expressions for water retention and conductivity data. *Ground Water* 35:848–858.
- Miller, E.E., and R.D. Miller. 1956. Physical theory for capillary flow phenomena. *J. Appl. Phys.* 27:324–332.
- Milly, P.C.D., and P.S. Eagleson. 1987. Effects of spatial variability on annual average water balance. *Water Resour. Res.* 23:2135–2143.
- Mualem, Y. 1976. A new model for predicting the hydraulic conductivity of unsaturated porous media. *Water Resour. Res.* 12:513–522.
- Nielsen, D.R., J.W. Biggar, and K.T. Erh. 1973. Spatial variability of field-measured soil-water properties. *Hilgardia* 42:215–260.
- Robin, M.J.L., A.L. Gutjahr, E.A. Sudicky, and J.L. Wilson. 1993. Cross-correlated random field generation with the direct Fourier transform method. *Water Resour. Res.* 29:2385–2397.
- Russo, D. 1988. Determining soil hydraulic properties by parameter estimation: On the selection of a model for the hydraulic properties. *Water Resour. Res.* 24:453–459.
- Schaap, M.G., and F.J. Leij. 1998. Database-related accuracy and uncertainty of pedotransfer functions. *Soil Sci.* 163:765–779.
- Schuh, W.M., and R.L. Cline. 1990. Effect of soil properties on unsaturated hydraulic conductivity pore-interaction factors. *Soil Sci. Soc. Am. J.* 54:1509–1519.
- Sharma, M.L., and R.J. Luxmoore. 1979. Soil spatial variability and its consequences on simulated water balance. *Water Resour. Res.* 15:1567–1573.
- Smith, R.E., and B. Diekkruger. 1996. Effective soil water characteristics and ensemble soil water profiles in heterogeneous soils. *Water Resour. Res.* 32:1993–2002.
- van Genuchten, M.Th. 1980. A closed-form equation for predicting the hydraulic conductivity of unsaturated soils. *Soil Sci. Soc. Am. J.* 44:892–898.
- van Genuchten, M.Th., and D.R. Nielsen. 1985. On describing and predicting the hydraulic properties of unsaturated soils. *Ann. Geophys.* 3:615–628.
- Warrick, A.W., and T.-C.J. Yeh. 1990. One-dimensional, steady vertical flow in a layered soil profile. *Adv. Water Resour.* 13:207–210.
- Wosten, J.H.M., and M.Th. van Genuchten. 1988. Using texture and other soil properties to predict the unsaturated soil hydraulic functions. *Soil Sci. Soc. Am. J.* 52:1762–1770.
- Yates, S.R., M.Th. van Genuchten, A.W. Warrick, and F.J. Leij. 1992. Analysis of measured, predicted, and estimated hydraulic conductivity using the RETC computer program. *Soil Sci. Soc. Am. J.* 56:347–354.
- Yeh, T.-C.J. 1989. One-dimensional steady state infiltration in heterogeneous soils. *Water Resour. Res.* 25:2149–2158.
- Zaslavsky, D. 1964. Theory of unsaturated flow into a non-uniform soil profile. *Soil Sci.* 97:400–410.